Urban Forestry & Urban Greening xxx (xxxx) 129022

Contents lists available at ScienceDirect

Urban Forestry & Urban Greening

journal homepage: www.elsevier.com/locate/ufug

Original article

Sensitivity of urban tree leaf phenology to precipitation and temperature in a mediterranean climate city

Amy K. Dixon [a,*], Michael Alonzo [b], Dar A. Roberts [a], Joseph P. McFadden [a]

[a] Department of Geography, University of California Santa Barbara, CA 93106, United States
[b] Department of Environmental Science, American University, Washington DC 20016, United States

ARTICLE INFO

Keywords:
Urban Forest
Phenology
Mediterranean Climate
PlanetScope

ABSTRACT

Urban forests provide important services to residents such as reducing air pollution, decreasing storm water runoff, and mitigating temperature extremes. Many of these benefits are dependent on when and how long leaves are on the trees, which is determined by their leaf phenology. The timing of phenological events is expected to shift with climate change, but the direction and magnitude are still uncertain. In Mediterranean climate regions, precipitation has been shown to be an important environmental cue in natural ecosystems; however, it is unclear whether this also applies to urban landscapes where additional water resources are common. To investigate this process, we used high resolution PlanetScope satellite imagery from 2018 to 2024 to monitor more than 35,000 species-identified trees in Santa Barbara, California. We successfully detected seasonal NDVI changes of individual trees, including evergreen species which we validated with field observations. In our image time series, 81.8 % of the deciduous tree population and, notably, 69.1 % of the evergreen tree population had at least one annual phenology cycle that was detected. Overall, trees were sensitive to precipitation with spring rain delaying the end of the season by 2.25 d/cm on average across species. Warm fall temperatures delayed the green-up date whereas warm winter temperatures led to an earlier green-up. These results build upon methods to study the diverse urban forest of semi-arid climates and deepen our understanding of how changing climatic patterns may affect the leaf phenology of these species.

1. Introduction

Urban trees are an important aspect to functional and livable cities. Studies have shown that urban forests can reduce stormwater runoff, decrease air pollution, and mitigate the urban heat island effect through shading and evapotranspiration (Nowak et al., 2006; Xiao and McPherson, 2016; Ziter et al., 2019). The magnitude of the benefits provided by trees is strongly influenced by their leaf phenology, or the timing of recurring and seasonal life-cycle events. The transition between developmental phases, or phenophases, is triggered by environmental cues. In the context of climate change, when these events occur is expected to shift (Cleland et al., 2007; Peñuelas et al., 2002), altering when new leaf growth begins and how long trees retain their leaves. How these processes respond to environmental cues will affect the provision of ecosystem services as shifting leaf phenology can result in changes to carbon, water, and energy fluxes (Piao et al., 2008; Richardson et al., 2013, 2010). Understanding these changes will also become increasingly important as urban areas continue to grow and more people rely on the services provided by urban vegetation (Grimm et al., 2008).

Most of the fundamental work untangling the mechanistic relationship between environmental conditions and phenology has been done in natural ecosystems, particularly focusing on spring phenology (e.g., "green-up") of deciduous vegetation in temperate climates (e.g., Elmore et al., 2012; Richardson et al., 2013). The typical cues that trees need to transition from dormancy to bud burst may consist of meeting a chilling requirement, thermal warming through accumulated heating, and in some cases a photoperiod threshold (Brunner et al., 2017). However, these cues can vary greatly among species, climate, and phenophase. Mediterranean climate regions are unique in two important ways that affect leaf phenology. First, they experience relatively mild temperatures throughout the year. Second, most of the rainfall occurs in the winter months, which creates an offset between the timing of peak water availability and high solar radiation input during the summer growing season. Additionally, Mediterranean regions typically do not experience a freezing period in the winter. Because of these factors, water

* Correspondence to: 1832 Ellison Hall, UC Santa Barbara, CA 93106, United States.
E-mail address: amydixon@ucsb.edu (A.K. Dixon).

https://doi.org/10.1016/j.ufug.2025.129022
Received 1 March 2025; Received in revised form 12 August 2025; Accepted 20 August 2025
1618-8667/

availability has been shown to be a strong driver of phenology in Mediterranean climates (Peñuelas et al., 2004).

Urban forests in Mediterranean climate zones are usually more species rich and diverse compared to those in other regions and include many non-native species that originate from other climate zones (Jenerette et al., 2016; Pincetl et al., 2013). Additionally, a large fraction of the vegetation is planted, as opposed to naturally grown. Socioeconomic factors, such as median household income or average building age, have been shown to be a main driver of diversity in semi-arid regions such as Southern California (Avolio et al., 2015). To further complicate this landscape, irrigation, management practices, and a wide range of urban microclimates may introduce variability to the phenology of city trees not seen in natural areas. For instance, cities have been associated with earlier springs and later end-of-season dates when compared to their surrounding non-urbanized regions due to the urban heat island effect (Melaas et al., 2016; Meng et al., 2020; Oke, 1982). However, the impact of urbanization on leaf phenology also depends on the background climate (Li et al., 2019), emphasizing the need for further research in Mediterranean climate cities.

While urban phenology studies have been done in the past, they have generally been through direct observations. Studies at the species level using remote sensing have been limited by the heterogeneity of the urban surface as well as the need for frequent monitoring to track phenology (Fang et al., 2020; Jensen and Cowen, 2011). Widely used data sources such as MODIS (500 m) can encompass more than 16 city blocks in a single pixel, and Landsat (30 m) pixels will often still contain a mixture of tree canopies, understories, and constructed surfaces (Wetherley et al., 2017). The relatively coarse spatial resolution of these data makes it difficult or impossible to reliably study the phenology of individual trees in urban landscapes.

New commercial datasets can fill this data gap as constellations of small satellites (e.g., PlanetScope) offer near-daily imagery of the Earth's surface at high spatial resolutions. These data can resolve many of the mature trees in cities and reduce uncertainty caused by mixed pixels (Zhao et al., 2022). With these characteristics, high spatial resolution imagery offers the ability to discriminate phenological patterns among species and functional types across an entire city.

Previous studies have shown the efficacy of using PlanetScope imagery to study phenological events of individual trees (see Alonzo et al., 2023; Pan et al., 2025; Wang and Gong, 2024), but have focused on deciduous species in non-Mediterranean climate regions. While Mediterranean climate regions cover a small fraction of earth's land surface, they are experiencing rapid urbanization with approximately 250 million people globally currently living in these areas (Gridded World Population v4, 2018). Additionally, as far as we are aware, there is no established method for monitoring evergreen leaf phenology of urban trees using a satellite remote sensing approach. To address this methodological and knowledge gap, we asked the following questions:

- How reliably can we use satellite imagery to study the leaf phenology of a mixed evergreen and deciduous urban forest?
- How do different climatic cues influence the timing of urban forest leaf phenology in a Mediterranean climate city, and is this species dependent?

To address these questions, we used a multi-year time series of high resolution PlanetScope imagery to understand the phenological and climatic relationships found in an urban, Mediterranean climate ecosystem. This study was conducted over the city of Santa Barbara, California, USA, using more than 35,000 individual and species-identified tree crowns where both evergreen and deciduous leaf phenology was monitored. We calculated phenological metrics for each tree between the years of 2019 and 2023 and then used linear regression modeling to estimate the phenological response to climatic conditions at the species-level.

2. Materials and methods

2.1. Study area

Santa Barbara is a coastal city with a population of ~88,000 (United States Census Bureau, 2020). The study area covers approximately 51 km^2 of the central business district extending from the coastline to the lower foothills of the nearby Santa Ynez Mountain range (Fig. 1). Included in the study area are a variety of land-use types such as commercial districts, residential areas, city parks, and unmanaged parcels. Santa Barbara has a Mediterranean climate (Köppen Csb) with a majority of the precipitation occurring in the winter season. The annual average rainfall and air temperature is 43 cm and 15 °C, respectively. A long history of horticulture has led to a diverse urban forest with a composition of over 450 species within the city (City of Santa Barbara Parks & Recreation), with many introduced non-native species and varying plant functional types (e.g. broadleaf, needleleaf, evergreen, deciduous). Vegetation in the city is supported by automated irrigation systems, especially in the summer dry season, but this is mostly for herbaceous ground cover. Other than juveniles, trees are generally not directly irrigated but sometimes have access to additional water resources from runoff or overirrigation.

2.2. Tree crown dataset

We used a previously created map of species-identified tree crown-objects produced from a fusion of privately collected Light Detecting and Ranging (lidar) data and hyperspectral Airborne Visible/Infrared Imaging Spectrometer (AVIRIS) data collected by NASA Jet Propulsion Laboratory (Fig. 1) (Alonzo et al., 2014). Airborne lidar data collected in 2010 with a point density of 22 points/m^2 were used to segment individual tree crowns. The structural and spectral information from the lidar and AVIRIS were then used to classify them into the 29 most common species found in Santa Barbara. This mapped trees from across the entire city including public streets, private residences, parks and gardens, and unmanaged parcels. The data had an overall classification accuracy of 83.4 % by total canopy area (Alonzo et al., 2014); however, there was variation in the species-specific accuracy. To reduce inclusion of misclassified trees, only species with a combined average producer's and user's accuracy > 75 % were included. Canopies with an area < 36 m^2 were removed to accommodate the 3 m resolution and 2.6 m nominal positional uncertainty of PlanetScope imagery (Alonzo et al., 2023, p. 5). To account for trees that had died or were removed since the original 2010 lidar collection, a normalized digital surface model created from 2018 lidar data (22.1 points/m^2) was used to screen out tree crowns that had an average height less than 2 m in 2018. After these data filtering steps, the species map we used contained 35,914 individual tree crowns across 20 species (Table 1).

2.3. PlanetScope imagery and processing

Planet operates the PlanetScope constellation of > 100 small satellites, or "Doves," capturing near-daily imagery of the entirety of Earth's land surface. There is overlap between the image scenes from the various sensors, but there is no organized tiling or grid system. Therefore, for any given date, the study area may be fully captured by a single scene, have multiple scenes from the same or different satellites, or only be partially imaged. We used the PlanetScope Surface Reflectance product, which has a nominal spatial resolution of 3 m consisting of four bands sampling red, green, blue, and near-infrared (NIR) wavelengths.

All available archived imagery that overlapped any portion of the study area with less than 10 % of cloud cover and a view-angle < 3 degrees was downloaded using Planet's API from January 1st, 2018 to May 8th, 2024 ($n = 1178$ images). Image processing and analysis was done using scripts written in R Statistical Software to automate the

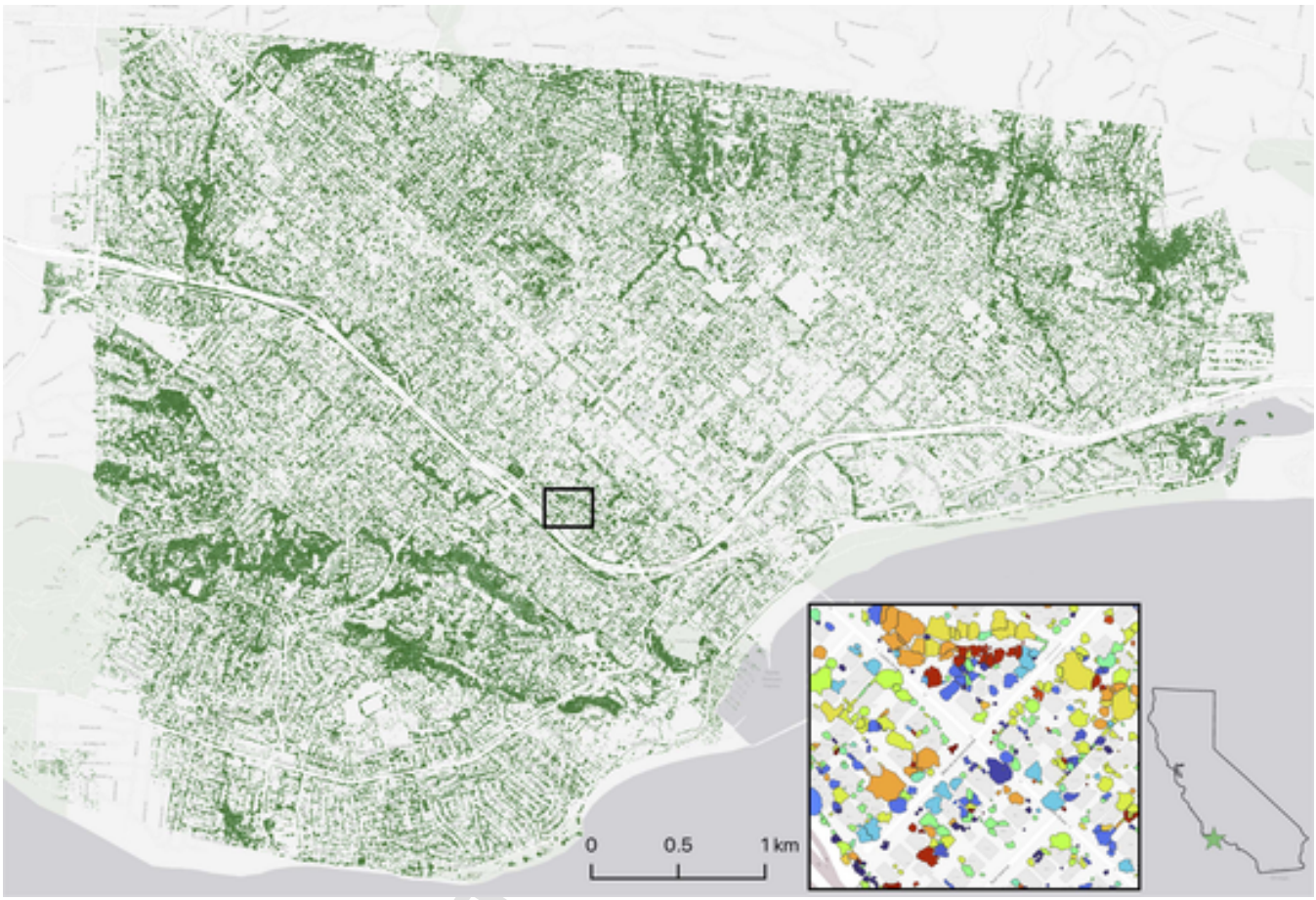

Fig. 1. Map of Santa Barbara and the tree crown dataset in green. The zoomed inset shows the individual tree crown polygons with colors representing different species classifications.

Table 1
Species used, abbreviated codes, and the number of individuals included in the study. An asterisk next to a species name indicates a deciduous species with all other species being evergreen.

Species Name	Species Code	n
Cinnamomum camphora	CICA	1595
Cupressus macrocarpa	CUMA	1241
Eucalyptus ficifolia	EUFI	1739
Eucalyptus globulus	EUGL	1471
Ficus microcarpa	FIMI	390
Geijera parviflora	GEPA	575
*Jacaranda mimosifolia**	JAMI*	2104
*Liquidambar styraciflua**	LIST*	1262
Magnolia grandiflora	MAGR	1154
Olea europaea	OLEU	855
Phoenix canariensis	PHCA	776
Pinus pinea	PIPI2	1198
Pittosporum undulatum	PIUN	3603
*Platanus racemosa**	PLRA*	1833
Podocarpus gracilior	POGR	1080
Quercus agrifolia	QUAG	11071
Schinus terebinthifolius	SCTE	1213
Syzygium australe	SYAU	535
*Tipuana tipu**	TISP*	1117
*Ulmus parvifolia**	ULPA*	1102
	Total	**35914**

process (v4.2.1, R Core Team, 2022). Each PlanetScope image is distributed with a Usable Data Mask that classifies all pixels as Clear, Cloud, Cloud Shadow, Haze, or Snow. Only Clear pixels were used, and all other classes were masked out.

To filter out images that were poorly georegistered, invariant targets (n = 76) throughout the study area were identified using National Agriculture Imagery Program aerial images. Targets were chosen such that there was high contrast in the NIR reflectance between the target and the surrounding area (e.g., asphalt from a school yard that is surrounded by lawn). For every image in our time series, the average reflectance values of the invariant targets were regressed against the reflectance values obtained from a high quality PlanetScope image that was chosen as the reference image (June 15th, 2022). Any image that had an $R^2 < 0.85$ for the NIR band was flagged as having an unacceptable amount of georegistration error, as evidenced by the mixed pixel effect on the invariant target, and therefore was removed from further analyses.

For the remaining images, a relative line correction using a different set of pure-pixel targets (n = 63) was performed to radiometrically normalize each image to the reference image (Furby and Campbell, 2001). These targets differ from the previous ones in that the main criterion was to ensure the target only contained a single invariant and homogenous surface (e.g., flat roofs, wide roads). Images that had an $R^2 < 0.7$ in the NIR or did not contain > 3 targets to include in the regression were also removed. This two-step process helped filter poorly georegistered images, mitigate differences in reflectance attributed to changes in solar zenith angle or differing atmospheric conditions, and flag im-

ages that contained contaminated pixels (e.g., clouds, fog, sensor artifacts).

After these filtering and normalization steps, our dataset consisted of 800 images covering 540 unique dates between April 9th, 2018, and May 7th, 2024 (Fig. 2). Since a large portion of the 2018 calendar year was removed and 2024 was not a complete year, data from these years were only used to buffer the spline fits (described in Section 2.4) of 2019 and 2023, respectively. For the full calendar years included in the study (i.e., 2019–2023), trees were imaged an average of 87.5 times a year.

2.4. NDVI time series and phenometric derivation

The normalized difference vegetation index (NDVI) is an index that indicates the "greenness" of vegetation by measuring the difference between the NIR and red band reflectance (Rouse et al., 1974). NDVI is sensitive to both the number of leaves as well as the condition of the individual leaves and is commonly used to monitor leaf phenology as it can measure the greenness of the tree canopy throughout the year. We calculated NDVI across all images to create a time series for each individual tree crown using Eq. 1:

$$NDVI = \frac{NIR - Red}{NIR + Red} \quad (1)$$

where *NIR* and *Red* are the percentages of reflected NIR and red light, respectively, that were recorded in the pixels within each tree canopy. A value closer to 1 indicates a greener canopy compared to a lower value. Seasonal fluctuations in NDVI are expected to be greater for fully deciduous trees compared to evergreen species. However, evergreen species can also change seasonally, despite keeping leaves year-round, as they add new growth and shed old leaves.

The surfaces beneath the tree (e.g., understory vegetation, concrete, asphalt) may show through the canopy and contribute to the measured reflectance in satellite imagery. Therefore, we used the 75th percentile of NDVI pixel values of each crown to minimize noise (Alonzo et al., 2023). If multiple PlanetScope images were available for a tree on a given day, we used the NDVI value from the image that was acquired by the newest generation of PlanetScope sensors. If the images were acquired with the same generation, then the image with the highest R^2 value from the radiometric relative line correction was used. Finally, each time series was despiked with a running median window using 5 points and 2 standard deviations as the cutoff to further filter erroneous values.

To determine the dates that each phenophase occurred, or the "phenometrics", we fitted each NDVI time series using a penalized cubic smoothing spline (Bolton et al., 2020; Moon et al., 2021). While other fitting methods have been used in the literature (Elmore et al., 2012), spline fitting allows for more flexibility in ecosystems that are not as well-behaved as temperate deciduous leaf phenology. Each spline fit was done by calendar year using a buffer of 185 days before and after January 1st and December 31st, respectively. The imagery available for analysis in 2018 and 2024 were not complete calendar years, therefore we did not compute phenometrics for these two years. However, the data were still used to properly buffer the spline fitting procedures for the 2019 and 2023 calendar years.

Each yearly NDVI curve was then evaluated to identify phenological cycles using a similar algorithm to that used by Bolton et al. (2020). Briefly, the green-up phase was considered as the segment of the curve between the peak and the preceding minimum NDVI value. Similarly, the green-down phase was from the peak to the following minimum NDVI value. To note, our use of the term "green-down" to designate the full decreasing segment of the curve differs from how Elmore et al. (2012) use the term to refer to a summer specific decreasing segment. For a curve to be considered a true phenological cycle, both the green-up and green-down phases needed to have a sustained increase or decrease, respectively, of NDVI (>35 % of global amplitude change) and an absolute change in NDVI greater or equal to 0.08. If a curve was a true phenological cycle, the day of year (DOY) the curve first crossed 15 % of the NDVI amplitude in the green-up phase was considered the green-up event, and the green-down event was the DOY the curve first dips below 15 % of the green-down phase amplitude (Fig. 3). If the green-up or green-down events extended into the previous or following calendar years, the DOY values would count down from 1 or up from 365, respectively. Finally, the growing season length (GSL) was calculated as the number of days between the green-up and green-down.

2.5. Ground observations of evergreen leaf growth

The use of PlanetScope imagery to track the leaf phenology of a highly diverse urban forest, especially one composed primarily of evergreen species such as Santa Barbara, is a relatively new application of this dataset. Therefore, we carried out a small set of ground-based phenology observations to confirm that increases in satellite derived NDVI corresponded with leaf growth as opposed to other artifacts (e.g., sun-sensor geometry). This was done by comparing field observations to PlanetScope NDVI retrievals using trees located on the campus of University of California, Santa Barbara (UCSB).

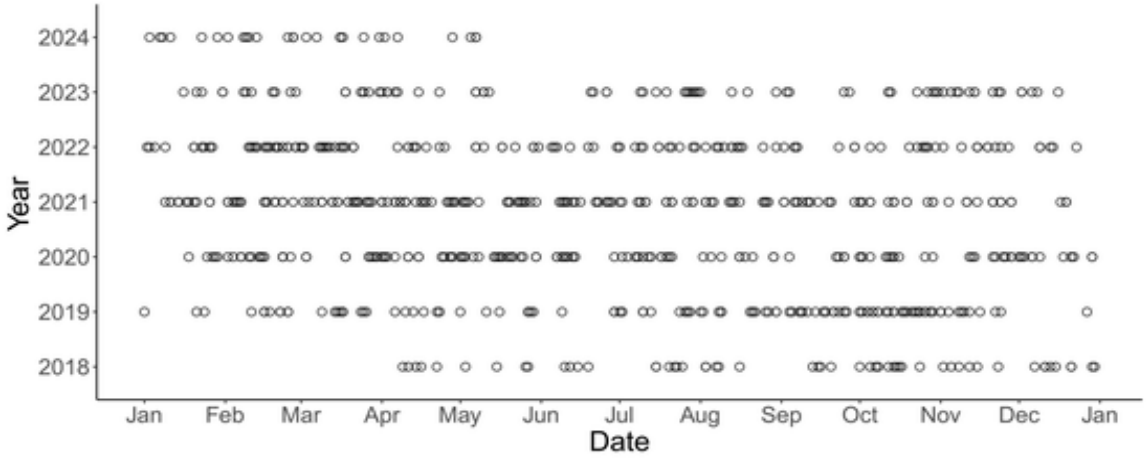

Fig. 2. Dates of available imagery that passed all quality checks (n = 800).

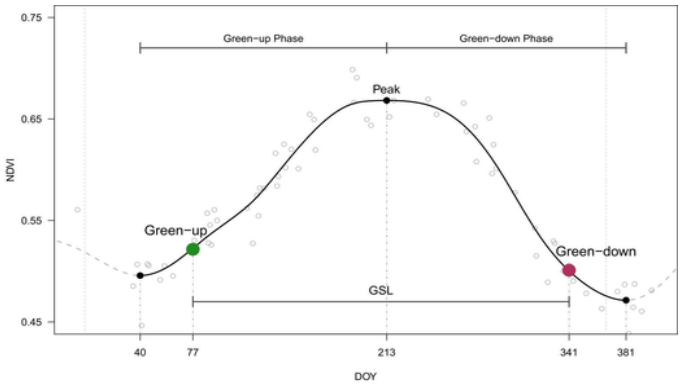

Fig. 3. An example of the method used to derive phenometrics (Green-up, Green-down, and GSL) of an individual PLRA tree for 2020.

Observations were collected for 27 trees of 7 different species (6 evergreens and 1 deciduous) 1–2 times a week during the green-up season in 2024 (February to May). For each observation, we estimated scores for each tree based on how much of the canopy area was composed of emerging and young leaves (i.e., 0 %, <1 %, 1–5 %, 5–10 %, 10–25 %, 25–50 %, and >50 %). When possible, trees were selected such that the tops of the canopies could be viewed from above from nearby buildings using binoculars, but many were also done from the ground. Similar NDVI calculations and phenometric processing was performed for this group of trees using PlanetScope imagery covering UCSB's campus. However, only the green-up phenometric was calculated as the field observations were only for leaf emergence.

While UCSB is not within the original project area, it hosts similar species as those found in the study. Additionally, these data were used to determine if NDVI changes in evergreens derived from the satellite imagery were based on real biological process (i.e., new leaf growth). Therefore, the different area coverage should not pose a significant problem for investigating this relationship.

2.6. Meteorological data and climate variables

We used Global Historical Climatology Network daily data from the National Centers for Environmental Information from a station in Santa Barbara (Station: USC00047902) to get daily air temperature and precipitation values during the study period (Fig. 4) (Menne et al., 2012). Notably, California went through a mega-drought between the years of 2012–2016, and drought conditions continued in Santa Barbara County until the end of 2018 (U.S. Drought Monitor, https://droughtmonitor.unl.edu). Winter precipitation between 2018 and 2019 alleviated the drought, but low precipitation between 2020 and 2022 resulted in another state of drought. Large amounts of precipitation followed in 2023 with more than 90 cm of rainfall during the water year (September 1 – August 31). Precipitation in 2024 was also relatively high with 77.3 cm of precipitation by the end of the study in May.

Climate variables included in the study were mean and maximum air temperature (TMEAN and TMAX, respectively), accumulated precipitation (PRCP), number of rain days (RD), growing degree days (GDD) and chilling units (CU). GDD and CU were calculated using Eqs. 2 and 3, respectively:

$$GDD = \begin{cases} \frac{T_{\min} + T_{\max}}{2} - T_{base}, & \frac{T_{\min} + T_{\max}}{2} > T_{base} \\ 0, & \frac{T_{\min} + T_{\max}}{2} < T_{base} \end{cases} \quad (2)$$

$$CU = \begin{cases} 1, & \frac{T_{\min} + T_{\max}}{2} < T_{base} \\ 0, & \frac{T_{\min} + T_{\max}}{2} > T_{base} \end{cases} \quad (3)$$

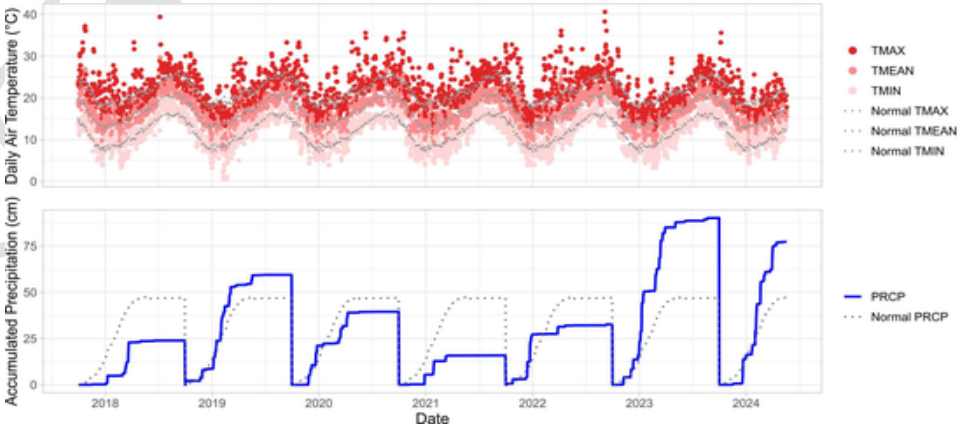

Fig. 4. Daily temperature and precipitation for Santa Barbara from Global Historical Climatology Network data. Red dots represent the maximum, mean, and minimum air temperature (TMAX, TMEAN, and TMIN, respectively). The blue line shows the accumulated precipitation (PRCP) calculated from the beginning of each water year (October 1st – September 30th). Grey dotted lines represent the 30-year normal values graphed over each year.

where T_{min} is the minimum daily air temperature, T_{max} is the maximum daily air temperature, and T_{base} is a threshold value to use as a cut-off for GDD and CU calculations. A value of 10˚C was used for T_{base} in this study, which is within the range of values used in the literature (Dantec et al., 2014; Didevarasl et al., 2023). Each climate variable was summed (GDD, CU, RD, PRCP) or averaged (TMEAN, TMAX) across different calendar months to estimate which periods of the year may be more important for driving phenology (e.g., accumulated winter precipitation or average summer month air temperature). A list of the variables used is shown in Table 2.

2.7. Statistical analysis of phenology and climate relationships

To understand the sensitivity of leaf phenology to environmental factors, we performed simple linear regressions on an individual tree basis to estimate the relationship of phenophase timing and climatic variables over the 5-year study. For example, the green-up DOYs for a tree would be regressed against the accumulated winter precipitation values for each corresponding year. The regressions used green-up, green-down, or GSL as the dependent variable and a climate variable as the independent variable. Only trees that had 3 or more detected phenological cycles were used in these regressions. Because some phenology–climate combinations did not follow a logical time sequence (i.e., climate variables at time points after a given phenological event), not all possible combinations were used (Table 2).

To understand the species-level response, the Pearson correlation coefficient was calculated for all trees with a linear regression model p-value < 0.1 and then averaged across individuals by species. The regression line slopes for these trees were also averaged together to determine the sensitivity of the phenology event timing to each climate variable by species. The p-value criterion decreased the number of individual trees in our climate analysis, an effect which was both species- and combination-specific. However, we also examined the climate correlation values without employing a regression p-value criterion and found similar patterns among species in terms of the direction of climate effects (i.e., earlier or later phenophase dates), but with weaker magnitudes. Therefore, we were confident that reducing the set of trees by the regression p-value criterion did not change our overall conclusions about the climate relationships.

Table 2
The climate variable, combination of months, and the phenophases used. Month combinations refer to January (1) through December (12) starting with the fall months of the preceding calendar year. An "X" marks whether that climate variable was regressed against the green-up, green-down, and growing season length (GSL).

Climate Variable	Months	Green-up	Green-down	GSL
Growing Degree Days (GDD)	11, 12	X		X
	11, 12, 1	X		X
	12, 1	X		X
	1, 2	X		X
	12, 1, 2	X		X
	11, 12, 1, 2	X		X
Chilling Units (CU)	11, 12	X		X
	11, 12, 1	X		X
	12, 1	X		X
	1, 2	X		X
	12, 1, 2	X		X
	11, 12, 1, 2	X		X
Precipitation and Number of Rain Days (PRCP, RD)	Water year (wy)		X	X
	12, 1, 2 (winter)	X	X	X
	10, 11, 12, 1, 2 (fall + winter)	X	X	X
	3, 4, 5 (spring)		X	X
Mean and Maximum Air Temperature (TMEAN, TMAX)	5, 6, 7		X	X
	6, 7		X	X
	5, 6, 7, 8		X	X
	6, 7, 8		X	X
	7, 8		X	X

3. Results

3.1. Comparison of satellite signal with field observations of leaf emergence

New leaf growth of evergreen trees as observed on the ground was detectable from the PlanetScope imagery. Of the 27 trees observed, 19 showed agreement between the ground and satellite observations. Of those 19 trees, 10 showed substantial leaf growth and a corresponding increase in NDVI (Fig. 5, QUAG). Some species had smaller fluctuations of NDVI increases during periods of new leaf growth (Supplemental Figure 1). The other pattern displayed by the remaining 9 trees was no observed growth coupled with no change in NDVI (Fig. 5, MAGR). This was seen in all MAGR and most of the FIMI trees. The remaining trees did not show a consistent pattern between observable leaf growth and changes in NDVI. All four of the *Pinus canariensis* trees, a species in the original tree crown dataset that was removed, showed a decrease in NDVI while new needles were growing (Supplemental Figure 1). There were also FIMI trees that had recorded new leaf growth, but did not show a reliable increase in NDVI while the new growth occurred.

To use as a point of reference, a winter deciduous tree (PLRA) was also observed in which the timing of new growth was almost perfectly synchronized between the ground and satellite observations (Fig. 5, PLRA). The difference between the fully bare and fully leafed-out PLRA canopy was an approximate change in NDVI of + 0.3. For the ever-

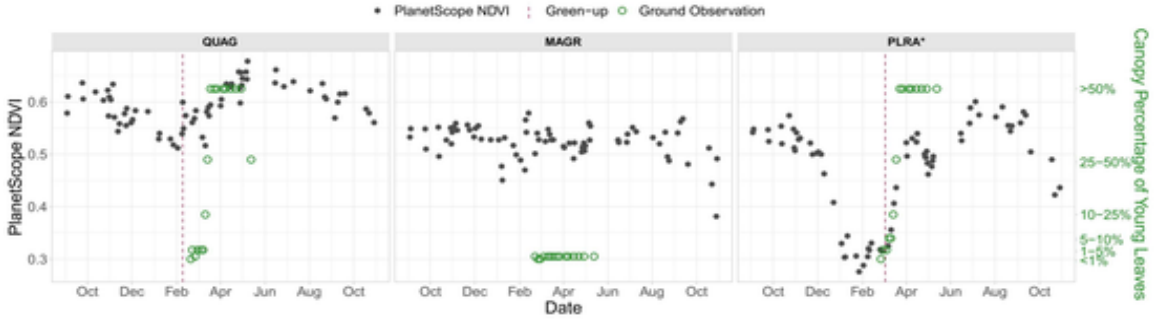

Fig. 5. PlanetScope calculated NDVI values (black) plotted with the field-collected ground observations (green) of the estimated percentage of new or young leaves from UCSB trees. The trees are shown as examples of the main patterns found; QUAG shows an evergreen increase in NDVI when leaf emergence was seen, MAGR is an evergreen tree that did not have any new leaf growth observed or an increase in NDVI, and PLRA is a deciduous tree where the timing of leaf emergence and an NDVI increase were very well timed. The dashed line (red) indicates the calculated green-up date from the NDVI time series.

green species that did show growth, the NDVI changes were closer to + 0.1 or + 0.2. Among the evergreen trees observed, QUAG was consistently well-timed between the two measures of increasing NDVI and observable new growth.

3.2. Phenological differences among functional types and species

We found that both evergreen and deciduous species had detectable phenological cycles in our time series of PlanetScope imagery. While 81.8 % of the total deciduous population exhibited a true phenological cycle, 69.1 % of the evergreen trees also had at least one year where a cycle was detected. During any given year, the proportion of trees with detected phenology cycles averaged to 59.3 % for deciduous and 33.5 % for evergreens. QUAG was the most seasonal of the evergreen species with 70 % of the population having a phenological cycle each year on average. EUGL followed with a yearly average of 43 % of the population. PHCA and OLEU were the least likely to have a phenological cycle with 20.5 % and 21.7 % of the population on average showing a true phenological cycle, respectively.

Species-specific leaf phenology patterns were also clearly identifiable in the time series of satellite imagery. On average, most species had green-up dates between January and February (Table 3). However, JAMI and TISP, two deciduous species that are known to drop their leaves late into winter or early spring, had an average green-up of 120.5 (SD = 53.3) and 101.5 (SD = 50.0), respectively. EUGL also stood out as one of the earlier species to green-up with an average green-up of 5.9 (SD = 54.4).

Green-down generally fell between September and December except for JAMI and LIST, which had average DOYs of 423.7 (SD = 68.9) and 399.1 (SD = 72.3), respectively. Interestingly, the GSL across species was relatively similar in length. The range of GSLs varied from 275.8 (CUMA, SD = 53.8) to 303.2 days (JAMI, SD = 40.9), with a total average across species and years being 288 days (SD = 41.9). These findings indicate that there is more variability among species in the timing of seasonal growth compared to the length of the growing season itself.

Due to these phenological differences, species can be further categorized into more specific groups. Of the deciduous species included in the study, JAMI and TISP stood out from the others as spring or late deciduous species, keeping their leaves on through the winter, whereas the others dropped their leaves earlier. Among the evergreen species, QUAG and EUGL stood out as synchronous and seasonal evergreen species. This can be seen by the high proportion of their populations having phenological cycles each year and the smaller variability in phenophase timing (Table 3, Supplemental Table 1). Other evergreens, however, were less seasonal and/or asynchronous in timing. For instance, PHCA had both low numbers of individuals with yearly phenological cycles and a wide spread of the timing of green-up and green-down. While OLEU also had low proportions of the population with phenological cycles, the spread of the timing was smaller than that of PHCA.

Table 3
Species average DOY (SD) for the green-up and green-down phenophases and the GSL in days. These values include all detected phenological cycles from every year averaged by species. An asterisk next to a species name indicates a deciduous species with all other species being evergreen.

Species	Green-up	Green-down	GSL
CICA	51 (63.9)	336.1 (74.6)	285.1 (43.8)
CUMA	14.4 (65.7)	290.3 (81.2)	275.8 (53.8)
EUFI	54.9 (62.1)	337.3 (75.8)	282.4 (46.8)
EUGL	5.9 (54.4)	281.9 (68.2)	276 (54.3)
FIMI	58.3 (51.7)	340.5 (65.5)	282.2 (49)
GEPA	40.6 (62.6)	327.9 (79.4)	287.3 (46.9)
JAMI*	120.5 (53.3)	423.7 (68.9)	303.2 (40.9)
LIST*	58.7 (58.3)	344.8 (71.4)	286.1 (41.3)
MAGR	39.4 (54)	320.2 (66.5)	280.8 (45.5)
OLEU	20.4 (59)	302.7 (72.6)	282.3 (47.9)
PHCA	20.9 (78.2)	306.2 (87.4)	285.2 (56.9)
PIPI2	15.7 (55.3)	298.1 (67.2)	282.4 (49.7)
PIUN	35.3 (55.9)	321.2 (62.8)	285.9 (44.4)
PLRA*	50.3 (39.8)	336.5 (46)	286.1 (35.1)
POGR	45.8 (61)	331.1 (67.9)	285.3 (45)
QUAG	23.8 (32.3)	312.2 (38.2)	288.4 (37)
SCTE	43.5 (63.2)	327.3 (75.3)	283.8 (50.9)
SYAU	43.5 (45.9)	324.2 (54.3)	280.7 (43.4)
TISP*	101.5 (50)	399.1 (72.3)	297.6 (45.2)
ULPA*	35.4 (42.7)	319.8 (54.1)	284.4 (42.8)

3.3. Spring green-up climatic drivers

Temperature as a driver of green-up was inconsistent across species and months. GDD and green-up had a mostly positive relationship across species (with the exceptions of JAMI, PHCA, and TISP) during late fall and into winter (Fig. 6, Green-up GDD.11.12 and GDD.12.1). This positive correlation indicates that a warmer temperature going into winter delays the green-up date. However, when looking just at the winter temperature (January and February, Green-up GDD.1.2), more species responded to warmer temperatures with earlier leaf emergence (i.e., a negative correlation). The average rate across all individuals was −0.063 d/GDD, but there was variability across species (Fig. 7). Deciduous species had an average rate of −0.238 d/GDD whereas the evergreen species average was 0.012 d/GDD, changing sign. CU showed similar but opposite patterns to GDD (Fig. 6, Supplemental Table 2).

Species also showed different responses to fall and winter precipitation. All the deciduous species had a positive correlation with higher amounts of fall and winter rain delaying the start of their season (Fig. 6, Green-up PRCP.fall.winter). PLRA had the highest positive rate of 1.359 d/cm of fall and winter precipitation (Fig. 7). Evergreen species were more variable. Interestingly, the species with negative correlations or rates were all evergreen species from native ranges with drier climates. However, many of the other evergreen species had a positive relationships, some of which also natively come from drier climates.

3.4. Climatic drivers of green-down events

Precipitation had a clear effect on the timing of the green-down phenophase. Increased precipitation during all time periods examined delayed leaf senescence and leaf drop across species with the exception of EUGL (Fig. 6). However, precipitation during the spring had the highest overall rate of extending the date of green-down compared to fall and winter precipitation (2.25 and 0.70 d/cm, $p < 0.001$). This was true for both deciduous and evergreen species. JAMI was the most sensitive with an average rate of 3.25 d/cm of spring precipitation followed by OLEU with a rate of 3.19 d/cm of precipitation (Fig. 7).

The direction of the relationship between green-down and average air temperature during the growing season depended on the time period and species. For most, warmer temperatures through summer meant an earlier green-down date, but the opposite was true when only looking at late summer month temperatures (i.e., July and August) (Fig. 6, Green-down TMEAN.7.8 and TMAX.7.8).

3.5. Interannual variation of phenology throughout the study period

Differences among years can be seen in both the green-up and green-down dates for different species (Fig. 8, Supplemental Table 1). Generally, the green-up distribution for many species shifts earlier in the year from 2019–2023 and green-down distributions shift later leading to elongated GSLs. The average GSL from all individuals was 272, 296, 273, 290, and 304 days for 2019 through 2023, respectively (Supplemental Table 1). An ANOVA test showed that the average GSLs for each year were significantly different from each other, and a *post hoc*

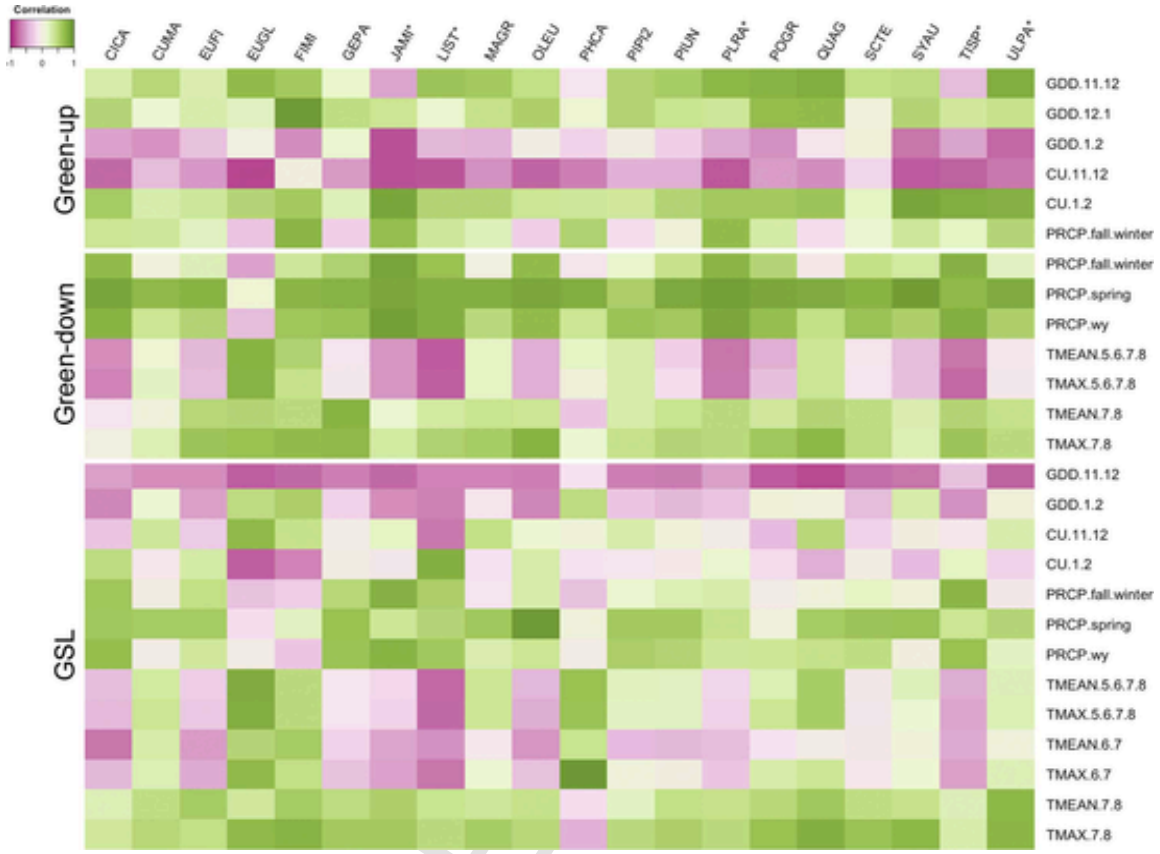

Fig. 6. Pearson correlation coefficients of phenophase and climate variable combinations. Each box represents the species average from all individuals that had a model p-value < 0.1. An asterisk next to a species name indicates a deciduous species with all other species being evergreen.

Tukey's Honestly Significant Difference test showed that all years were significantly different from each other.

4. Discussion

4.1. PlanetScope imagery to track urban and evergreen leaf phenology

This research supports previous work that PlanetScope imagery can capture the heterogeneous landscape of urban forests and their seasonality (Alonzo et al., 2023; Wang and Gong, 2024); however, as far as we are aware, our study is the first to have a large focus on urban evergreen leaf phenology. The evergreen-dominated urban forest we studied showed distinct seasonality of leaf emergence and leaf turnover in the satellite imagery, a phenomenon that has also been observed in tropical evergreen forests (Huete et al., 2006). The agreement we found between the satellite NDVI and new leaf growth observed in the field supports a meaningful biophysical interpretation of evergreen seasonality. Here we attribute the seasonal fluctuations of NDVI in evergreen trees to the emergence and maturation of new leaves (Luo et al., 2022; Wu et al., 2018).

There was variation among species in how likely an evergreen individual would have a phenological cycle. One explanation could be that species showing fewer phenological cycles are more aseasonal in their leaf turnover habits and therefore do not show large changes in NDVI throughout the year. Additionally, there is likely a species-specific spectral and structural difference in new growth that makes certain species more or less likely to show fluctuations in NDVI. This could account for why some of the trees observed in the field had the opposite pattern between NDVI changes and leaf growth. On the other hand, QUAG had the highest proportion of the population showing yearly seasonality which is supported by an established period of leaf growth for this species (Munz and Keck, 1973). It is also possible that the normal phenological habits of species in their native ranges and climates will change in a novel Mediterranean climate region.

There are differences in the magnitude of seasonal NDVI fluctuations between evergreen and deciduous trees. Therefore, adjustments may be required to accurately detect seasonal cycles when studying a mixed forest (Li et al., 2023). While there is still more work to be done in understanding evergreen leaf phenology, this study shows promising results to better understand the complexities of using optical remote sensing for evergreen leaf phenology.

4.2. Precipitation effects on green-down and GSL

Previous studies have shown that increased rainfall lengthens the growing season in natural areas that are water-limited (Liu et al., 2016; Mazer et al., 2015; Peñuelas et al., 2004), as well as in experimental set ups (Bao et al., 2020); however, it was unclear whether this would hold true in an urban area where irrigation can provide valuable water resources to trees. Our results showed that overall precipitation extended the green-down date across all species. GSL was also highly positively correlated with precipitation for all time periods of the year, which is likely a downstream effect of a delayed green-down. This relationship is exemplified in 2023 when accumulated precipitation was unusually high and the average green-down dates were the latest during the study across most species. These results may imply that under drought conditions, which can also come with warmer temperatures, it could be beneficial to dedicate water resources for trees to promote growth and extend the length of the growing season.

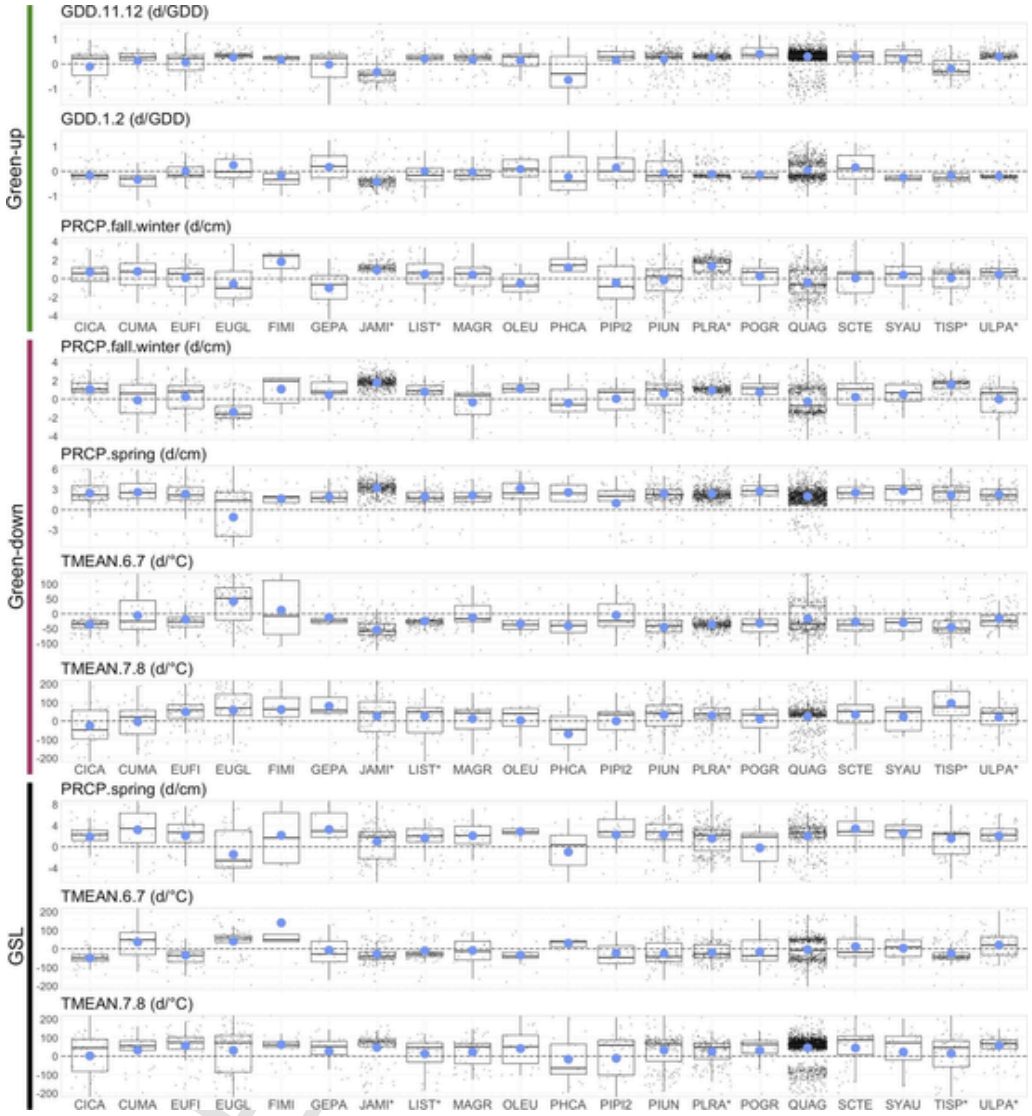

Fig. 7. Slope values of linear regression models for selected phenophase and climate variable combinations by species. The blue point represents the average value. For visualization purposes, the axis scales have been limited to show the central data with some outliers being cut-out from the graphs.

That being said, many of the trees that showed delayed green-down dates from spring precipitation were located on unmanaged parcels or next to creeks that run through the city. There were street and residential trees that also showed a strong positive relationship as well, but they were fewer in number. Work in a desert city showed that urban vegetation was decoupled from precipitation cues the nearby natural desert vegetation responded to (Buyantuyev and Wu, 2012). It is possible irrigation of park and residential trees and additional water from runoff is reducing water-stress and making these trees less sensitive to precipitation patterns. However, this is hard to confirm without having city-wide irrigation data available. Future research could investigate this relationship more closely with the potential to use this to map which trees are or are not receiving additional water resources.

4.3. Temperature effects on phenology

Warmer temperatures in winter have been shown to lead to earlier green-up dates (Liu and Zhang, 2020; Meng et al., 2020), and this was also seen in our study across species and functional types when only looking at the temperatures of January and February. However, GDD of earlier months from November through January had a positive correlation with green-up, meaning later green-up dates with warmer temperatures. Interestingly, the green-up dates of this study are relatively earlier than those reported in other temperate climate study areas (Alonzo et al., 2023; Melaas et al., 2013; Moon et al., 2021). This difference may indicate that the relatively mild Mediterranean climate induces an earlier spring and shorter winter seasons. It has been shown that the background climate is an important factor when trying to understand phenology and climate relationships (Li et al., 2022), and urban phenology across Mediterranean climate regions has more variability compared to temperate climate cities (Galán Díaz et al., 2023). This may be a contributing factor as to why some species in this study are showing a positive relationship with accumulated GDD when many natural ecosystems have shown negative relationships (Elmore et al., 2012; Richardson et al., 2013).

The varying responses to summer temperatures and the effect on green-down could be attributed to water stress during the summer dry period (Liu et al., 2016). Warming has been shown in boreal forests to advance the start of spring leading to an earlier depletion of soil moisture and earlier green-down dates (Buermann et al., 2013). It is possible that a similar process occurs in our study area; however, when the late summer period was warmer there was generally a delay in leaf senes-

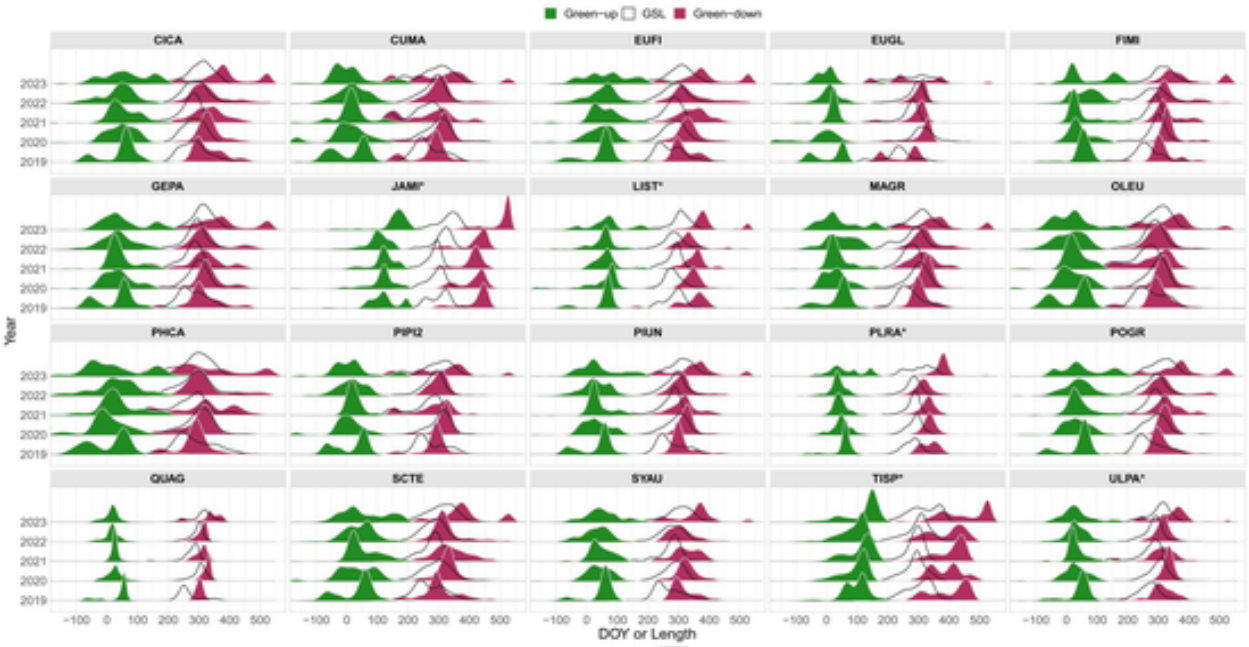

Fig. 8. Density histograms of the Green-up (green) and Green-down (red) DOY as well as the GSL (black) in days from all detected phenological cycles separated by year and species. An asterisk next to a species name indicates a deciduous species with all other species being evergreen.

cence and leaf drop. This work could benefit from a longer time series to develop a fuller understanding of temperature effects on urban trees in our Mediterranean climate city.

4.4. Phenological variability among species

The phenological timing of green-up and green-down was more variable among species than was the overall length of the growing season. We did find interannual differences in GSL, but they were relatively conserved across species, and phenophase timing from our study are similar to other studies in this region (Bolton et al., 2020; Li et al., 2017). This has implications for using phenology as an attribute for species classification (e.g., timing of green-up) methods as well as the structural function of the urban forest. Deciduous trees on average had a longer GSL than evergreens calculated by the methods in this paper (6.7 days, $p < 0.001$, Supplemental Table 1), but evergreen species retain leaves for most or all of year, and thus provide ecosystem services such as evapotranspiration and shade related cooling during periods when deciduous trees are dormant.

There was also a large amount of variability within species of leaf phenology timing in this study, which can be seen by the large standard deviations of the phenometric dates (Table 3). The variability could also be a result of the mild climate found in Santa Barbara in that the seasonality of the background climate is not strong enough to drive a concerted timing of leaf growth or senescence within species populations. This suggests the microclimate within the urban landscape experienced by an individual tree, or the typical species plasticity, may be a source of variation we are seeing within species. Differences in management practices, such as tree pruning, could also account for some of the variability as pruning could be detected as a green-down event and may instigate new leaf growth independent of normal phenological cycles. However, these averages are also taken from multiple years which could be contributing to a wider spread of DOYs as each year had different climatic conditions.

4.5. Study limitations

This study presents a method for studying evergreen leaf phenology from a remote sensing approach and quantifies the phenological and climatic relationships of a Mediterranean climate urban forest. The ability to study individual tree crowns with high resolution satellite imagery opens many doors for urban forest research. While our ground observations generally aligned well with the satellite imagery, they did also show this could be highly species dependent, which could be due to factors such as structural, spectral, or physiological differences. This study documents a method for studying evergreen leaf phenology using high temporal and spatial resolution satellite imagery, and further applications of the method should confirm the species-specific compatibility.

While species-specific sensitivities to a suite of climatic variables are reported, it is important to note that phenology is regulated by complex signaling networks of both endogenous and environmental factors (Brunner et al., 2017). There are usually multiple cues involved, and they may not always interact linearly. Additionally, tree responses quantified under current conditions may not hold true under future extreme climate conditions or reflect tree adaptations to long-term stress.

Furthermore, the statistical analysis was conducted on a subpopulation of each species that showed marked NDVI seasonality (i.e., there was a detected phenology cycle) and then filtered by p-values based on each regression model. These values inherently cannot reflect the responses of the trees that did not have a detected phenology cycle. Additionally, some combinations had much smaller sample sizes and could be based on a biased population of the species. We did calculate the species averages without the extra p-filtering step, and generally found similar directional patterns; however, some combinations flipped signs of correlation and/or sensitivity values (Supplemental Table 2).

5. Conclusions

In this study, we answered two questions. First, we asked if leaf phenology of a diverse mixed urban forest is detectable using high resolution PlanetScope satellite imagery. We demonstrated that species-

specific leaf phenology patterns are identifiable using these data, including those of evergreen species. Second, we asked which climatic factors are important drivers of phenology in a Mediterranean climate city. We found that higher amounts of precipitation were highly correlated with delaying the green-down date and extending the growing season length. We also found that warmer air temperatures throughout the summer were associated with an earlier green-down, but higher temperatures specifically at the end of summer could delay the end of the season. Additionally, warmer temperatures during the late fall season led to later green-up dates, but higher winter temperatures resulted in earlier green-up dates. This research advances our knowledge of species-specific phenology and climate relationships and offers a new method for studying mixed urban forests.

CRediT authorship contribution statement

Roberts Dar A: Writing – review & editing, Methodology. **Michael Alonzo:** Writing – review & editing, Methodology, Conceptualization. **McFadden Joseph P:** Writing – review & editing, Methodology, Conceptualization. **Dixon Amy K:** Writing – review & editing, Writing – original draft, Visualization, Methodology, Investigation, Formal analysis, Data curation, Conceptualization.

Uncited reference

Center for International Earth Science Information Network - CIESIN - Columbia University 2018; City of Santa Barbara Parks & Recreation 2024; Rouse et al., 1973; United States Census Bureau 2019; https://www 2024; U.S. Drought Monitor 2024.

Declaration of Competing Interest

The authors declare that they have no known competing financial interests or personal relationships that could have appeared to influence the work reported in this paper.

Acknowledgements

This research did not receive any specific grant from funding agencies in the public, commercial, or not-for-profit sectors. We would like to thank the DREAM Lab for acquiring the license with Planet that allowed us to download imagery needed for this research. We would also like to thank three anonymous reviewers for their constructive comments and suggestions that helped improve the manuscript.

Appendix A. Supporting information

Supplementary data associated with this article can be found in the online version at doi:10.1016/j.ufug.2025.129022.

References

Alonzo, M., Baker, M.E., Caplan, J.S., Williams, A., Elmore, A.J., 2023. Canopy composition drives variability in urban growing season length more than the heat island effect. Sci. Total Environ. 884, 163818. https://doi.org/10.1016/j.scitotenv.2023.163818.

Alonzo, M., Bookhagen, B., Roberts, D.A., 2014. Urban tree species mapping using hyperspectral and lidar data fusion. Remote Sens. Environ. 148, 70–83. https://doi.org/10.1016/j.rse.2014.03.018.

Avolio, M.L., Pataki, D.E., Gillespie, T.W., Jenerette, G.D., McCarthy, H.R., Pincetl, S., Weller Clarke, L., 2015. Tree diversity in Southern California's urban forest: the interacting roles of social and environmental variables. Front. Ecol. Evol. 3. https://doi.org/10.3389/fevo.2015.00073.

Bao, F., Liu, M., Cao, Y., Li, J., Yao, B., Xin, Z., Lu, Q., Wu, B., 2020. Water addition prolonged the length of the growing season of the desert shrub nitraria tangutorum in a temperate desert. Front. Plant Sci. 11, 1099. https://doi.org/10.3389/fpls.2020.01099.

Bolton, D.K., Gray, J.M., Melaas, E.K., Moon, M., Eklundh, L., Friedl, M.A., 2020. Continental-scale land surface phenology from harmonized landsat 8 and Sentinel-2 imagery. Remote Sens. Environ. 240, 111685. https://doi.org/10.1016/j.rse.2020.111685.

Brunner, A.M., Varkonyi-Gasic, E., Jones, R.C., 2017. Phase change and phenology in trees. In: Groover, A., Cronk, Q. (Eds.), Comparative and Evolutionary Genomics of Angiosperm Trees. Springer International Publishing, Cham, pp. 227–274. https://doi.org/10.1007/7397_2016_30.

Buermann, W., Bikash, P.R., Jung, M., Burn, D.H., Reichstein, M., 2013. Earlier springs decrease peak summer productivity in north American boreal forests. Environ. Res. Lett. 8, 024027. https://doi.org/10.1088/1748-9326/8/2/024027.

Buyantuyev, A., Wu, J., 2012. Urbanization diversifies land surface phenology in arid environments: interactions among vegetation, climatic variation, and land use pattern in the Phoenix metropolitan region, USA. Landsc. Urban Plan 105, 149–159. https://doi.org/10.1016/j.landurbplan.2011.12.013.

Center for International Earth Science Information Network - CIESIN - Columbia University, 2018. Gridded population of the world. Version 4 (GPWv4): Population Count, Revision 11. NASA Socioeconomic Data and Applications Center (SEDAC), Palisades, New York.

City of Santa Barbara Parks & Recreation. Trees and Urban Forestry. [WWW document]. URL. ⟨https://sbparksandrec.santabarbaraca.gov/programs-services/trees-and-urban-forestry⟩, Accessed date: 04 August 2024.

Cleland, E., Chuine, I., Menzel, A., Mooney, H., Schwartz, M., 2007. Shifting plant phenology in response to global change. Trends Ecol. Evol. 22, 357–365. https://doi.org/10.1016/j.tree.2007.04.003.

Dantec, C.F., Vitasse, Y., Bonhomme, M., Louvet, J.-M., Kremer, A., Delzon, S., 2014. Chilling and heat requirements for leaf unfolding in european beech and sessile oak populations at the Southern limit of their distribution range. Int. J. Biometeorol. 58, 1853–1864. https://doi.org/10.1007/s00484-014-0787-7.

Didevarasl, A., Costa Saura, J.M., Spano, D., Deiana, P., Snyder, R.L., Mulas, M., Nieddu, G., Zelasco, S., Santona, M., Trabucco, A., 2023. Modeling phenological phases across olive cultivars in the Mediterranean. Plants 12, 3181. https://doi.org/10.3390/plants12183181.

Elmore, A.J., Guinn, S.M., Minsley, B.J., Richardson, A.D., 2012. Landscape controls on the timing of spring, autumn, and growing season length in mid-Atlantic forests. Glob. Change Biol. 18, 656–674. https://doi.org/10.1111/j.1365-2486.2011.02521.x.

Fang, F., McNeil, B.E., Warner, T.A., Maxwell, A.E., Dahle, G.A., Eutsler, E., Li, J., 2020. Discriminating tree species at different taxonomic levels using multi-temporal WorldView-3 imagery in Washington D.C., USA. Remote Sens. Environ. 246, 111811. https://doi.org/10.1016/j.rse.2020.111811.

Furby, S.L., Campbell, N.A., 2001. Calibrating images from different dates to 'like-value' digital counts. Remote Sens. Environ. 77, 186–196. https://doi.org/10.1016/S0034-4257(01)00205-X.

Galán Díaz, J., Gutiérrez-Bustillo, A.M., Rojo, J., 2023. The phenological response of european vegetation to urbanisation is mediated by macrobioclimatic factors. Sci. Total Environ. 905, 167092. https://doi.org/10.1016/j.scitotenv.2023.167092.

Grimm, N.B., Faeth, S.H., Golubiewski, N.E., Redman, C.L., Wu, J., Bai, X., Briggs, J.M., 2008. Global change and the ecology of cities. Science 319, 756–760. https://doi.org/10.1126/science.1150195.

Huete, A.R., Didan, K., Shimabukuro, Y.E., Ratana, P., Saleska, S.R., Hutyra, L.R., Yang, W., Nemani, R.R., Myneni, R., 2006. Amazon rainforests Green-up with sunlight in dry season. Geophys. Res. Lett. 33, 2005GL025583. https://doi.org/10.1029/2005GL025583.

Jenerette, G.D., Clarke, L.W., Avolio, M.L., Pataki, D.E., Gillespie, T.W., Pincetl, S., Nowak, D.J., Hutyra, L.R., McHale, M., McFadden, J.P., Alonzo, M., 2016. Climate tolerances and trait choices shape continental patterns of urban tree biodiversity. Glob. Ecol. Biogeogr. 25, 1367–1376. https://doi.org/10.1111/geb.12499.

Jensen, J.R., Cowen, D.C., 2011. Remote sensing of Urban/Suburban infrastructure and Socio-Economic attributes. In: Dodge, M., Kitchin, R., Perkins, C. (Eds.), The Map Reader. Wiley, pp. 153–163. https://doi.org/10.1002/9780470979587.ch22.

Li, D., Stucky, B.J., Baiser, B., Guralnick, R., 2022. Urbanization delays plant leaf senescence and extends growing season length in cold but not in warm areas of the Northern hemisphere. Glob. Ecol. Biogeogr. 31, 308–320. https://doi.org/10.1111/geb.13429.

Li, D., Stucky, B.J., Deck, J., Baiser, B., Guralnick, R.P., 2019. The effect of urbanization on plant phenology depends on regional temperature. Nat. Ecol. Evol. 3, 1661–1667. https://doi.org/10.1038/s41559-019-1004-1.

Li, R., Xia, H., Zhao, X., Guo, Y., 2023. Mapping evergreen forests using new phenology index, time series Sentinel-1/2 and google earth engine. Ecol. Indic. 149, 110157. https://doi.org/10.1016/j.ecolind.2023.110157.

Li, Xuecao, Zhou, Y., Asrar, G.R., Mao, J., Li, Xiaoma, Li, W., 2017. Response of vegetation phenology to urbanization in the conterminous United States. Glob. Change Biol. 23, 2818–2830. https://doi.org/10.1111/gcb.13562.

Liu, L., Zhang, X., 2020. Effects of temperature variability and extremes on spring phenology across the contiguous United States from 1982 to 2016. Sci. Rep. 10, 17952. https://doi.org/10.1038/s41598-020-74804-4.

Liu, Q., Fu, Y.H., Zhu, Z., Liu, Y., Liu, Z., Huang, M., Janssens, I.A., Piao, S., 2016. Delayed autumn phenology in the Northern hemisphere is related to change in both climate and spring phenology. Glob. Change Biol. 22, 3702–3711. https://doi.org/10.1111/gcb.13311.

Luo, Y., Pacheco-Labrador, J., Richardson, A.D., Seyednasrollah, B., Perez-Priego, O., Gonzalez-Cascon, R., Martín, M.P., Moreno, G., Nair, R., Wutzler, T., Bucher, S.F., Carrara, A., Cremonese, E., El-Madany, T.S., Filippa, G., Galvagno, M., Hammer, T., Ma, X., Martini, D., Zhang, Q., Reichstein, M., Menzel, A., Römermann, C., Migliavacca, M., 2022. Evergreen broadleaf greenness and its relationship with leaf flushing, aging, and water fluxes. Agric. For. Meteor. 323, 109060. https://doi.org/10.1016/j.agrformet.2022.109060.

Mazer, S.J., Gerst, K.L., Matthews, E.R., Evenden, A., 2015. Species-specific phenological responses to winter temperature and precipitation in a water-limited ecosystem.

art98. Ecosphere 6. https://doi.org/10.1890/ES14-00433.1.
Melaas, E.K., Friedl, M.A., Zhu, Z., 2013. Detecting interannual variation in deciduous broadleaf forest phenology using landsat TM/ETM+ data. Remote Sens. Environ. 132, 176–185. https://doi.org/10.1016/j.rse.2013.01.011.
Melaas, E.K., Wang, J.A., Miller, D.L., Friedl, M.A., 2016. Interactions between urban vegetation and surface urban heat islands: a case study in the Boston metropolitan region. Environ. Res. Lett. 11, 054020. https://doi.org/10.1088/1748-9326/11/5/054020.
Meng, L., Mao, J., Zhou, Y., Richardson, A.D., Lee, X., Thornton, P.E., Ricciuto, D.M., Li, X., Dai, Y., Shi, X., Jia, G., 2020. Urban warming advances spring phenology but reduces the response of phenology to temperature in the conterminous United States. Proc. Natl. Acad. Sci. 117, 4228–4233. https://doi.org/10.1073/pnas.1911117117.
Menne, M.J., Durre, I., Vose, R.S., Gleason, B.E., Houston, T.G., 2012. An overview of the global historical climatology Network-Daily database. J. Atmos. Ocean. Technol. 29, 897–910. https://doi.org/10.1175/JTECH-D-11-00103.1.
Moon, M., Richardson, A.D., Friedl, M.A., 2021. Multiscale assessment of land surface phenology from harmonized landsat 8 and Sentinel-2, PlanetScope, and PhenoCam imagery. Remote Sens. Environ. 266, 112716. https://doi.org/10.1016/j.rse.2021.112716.
Munz, P.A., Keck, D.D., 1973. A california flora and supplement. University of California Press, Berkeley, CA, p. 904.
Nowak, D.J., Crane, D.E., Stevens, J.C., 2006. Air pollution removal by urban trees and shrubs in the United States. Urban For. Urban Green. 4, 115–123. https://doi.org/10.1016/j.ufug.2006.01.007.
Oke, T.R., 1982. The energetic basis of the urban heat island. Q. J. R. Meteorol. Soc. 108, 1–24. https://doi.org/10.1002/qj.49710845502.
Pan, B., Xiao, X., Luo, S., Pan, L., Yao, Y., Zhang, C., Meng, C., Qin, Y., 2025. Identify and track White flower and leaf phenology of deciduous broadleaf trees in spring with time series PlanetScope images. ISPRS J. Photogramm. Remote Sens 226, 127–145. https://doi.org/10.1016/j.isprsjprs.2025.05.013.
Peñuelas, J., Filella, I., Comas, PerE., 2002. Changed plant and animal life cycles from 1952 to 2000 in the Mediterranean region. Glob. Change Biol. 8, 531–544. https://doi.org/10.1046/j.1365-2486.2002.00489.x.
Peñuelas, J., Filella, I., Zhang, X., Llorens, L., Ogaya, R., Lloret, F., Comas, P., Estiarte, M., Terradas, J., 2004. Complex spatiotemporal phenological shifts as a response to rainfall changes. N. Phytol. 161, 837–846. https://doi.org/10.1111/j.1469-8137.2004.01003.x.
Piao, S., Ciais, P., Friedlingstein, P., Peylin, P., Reichstein, M., Luyssaert, S., Margolis, H., Fang, J., Barr, A., Chen, A., Grelle, A., Hollinger, D.Y., Laurila, T., Lindroth, A., Richardson, A.D., Vesala, T., 2008. Net carbon dioxide losses of Northern ecosystems in response to autumn warming. Nature 451, 49–52. https://doi.org/10.1038/nature06444.
Pincetl, S., Prabhu, S.S., Gillespie, T.W., Jenerette, G.D., Pataki, D.E., 2013. The evolution of tree nursery offerings in Los Angeles county over the last 110 years. Landsc. Urban Plan 118, 10–17. https://doi.org/10.1016/j.landurbplan.2013.05.002.
R Core Team (2022). R: A Language and Environment for Statistical Computing. R Foundation for Statistical Computing, Vienna, Austria. ⟨https://www.R-project.org/⟩.
Richardson, A.D., Andy Black, T., Ciais, P., Delbart, N., Friedl, M.A., Gobron, N., Hollinger, D.Y., Kutsch, W.L., Longdoz, B., Luyssaert, S., Migliavacca, M., Montagnani, L., William Munger, J., Moors, E., Piao, S., Rebmann, C., Reichstein, M., Saigusa, N., Tomelleri, E., Vargas, R., Varlagin, A., 2010. Influence of spring and autumn phenological transitions on forest ecosystem productivity. Philos. Trans. R. Soc. B Biol. Sci. 365, 3227–3246. https://doi.org/10.1098/rstb.2010.0102.
Richardson, A.D., Keenan, T.F., Migliavacca, M., Ryu, Y., Sonnentag, O., Toomey, M., 2013. Climate change, phenology, and phenological control of vegetation feedbacks to the climate system. Agric. For. Meteor. 169, 156–173. https://doi.org/10.1016/j.agrformet.2012.09.012.
Rouse, J.W., Haas, R.H., Schell, J.A., Deering, D.W., 1973. Monitoring vegetation systems in the great plains with ERTS, In: Third ETS Symposium. NASA SP-351 1. NASA, Washington, DC, pp. 309–317.
United States Census Bureau, 2019. QuickFacts: Santa Barbara city, California [WWW document]. URL.
https://www.census.gov/quickfacts/fact/table/santabarbaracitycalifornia,US/POP010220, Accessed date: 04 August 2024.
U.S. Drought Monitor. National Drought Mitigation Center. [WWW document]. URL. ⟨https://droughtmonitor.unl.edu/CurrentMap/StateDroughtMonitor.aspx?fips_06083⟩, Accessed date: 04 August 2024.
Wang, H., Gong, F.-Y., 2024. Quantifying City- and Street-Scale urban tree phenology from Landsat-8, Sentinel-2, and PlanetScope images: a case study in downtown Beijing. Remote Sens 16, 2351. https://doi.org/10.3390/rs16132351.
Wetherley, E.B., Roberts, D.A., McFadden, J.P., 2017. Mapping spectrally similar urban materials at sub-pixel scales. Remote Sens. Environ. 195, 170–183. https://doi.org/10.1016/j.rse.2017.04.013.
Wu, J., Kobayashi, H., Stark, S.C., Meng, R., Guan, K., Tran, N.N., Gao, S., Yang, W., Restrepo-Coupe, N., Miura, T., Oliviera, R.C., Rogers, A., Dye, D.G., Nelson, B.W., Serbin, S.P., Huete, A.R., Saleska, S.R., 2018. Biological processes dominate seasonality of remotely sensed canopy greenness in an Amazon evergreen forest. N. Phytol. 217, 1507–1520. https://doi.org/10.1111/nph.14939.
Xiao, Q., McPherson, E.G., 2016. Surface water storage capacity of twenty tree species in davis, california. J. Environ. Qual. 45, 188–198. https://doi.org/10.2134/jeq2015.02.0092.
Zhao, Y., Lee, C.K.F., Wang, Z., Wang, J., Gu, Y., Xie, J., Law, Y.K., Song, G., Bonebrake, T.C., Yang, X., Nelson, B.W., Wu, J., 2022. Evaluating fine-scale phenology from PlanetScope satellites with ground observations across temperate forests in eastern North America. Remote Sens. Environ. 283, 113310. https://doi.org/10.1016/j.rse.2022.113310.
Ziter, C.D., Pedersen, E.J., Kucharik, C.J., Turner, M.G., 2019. Scale-dependent interactions between tree canopy cover and impervious surfaces reduce daytime urban heat during summer. Proc. Natl. Acad. Sci. 116, 7575–7580. https://doi.org/10.1073/pnas.1817561116.